The 2024 World Congress on
The 2024 Structures Congress (Structures24)
19-22, August, 2024, The K hotel, Seoul, Korea

Structural design of a reconfigurable and temporary spatial structure according to the Eurocodes

*Stefanos Gkatzogiannis[1)], Marios C. Phocas[2)] and Eftychios G. Christoforou[3)]

[1), 2)] *Department of Architecture, University of Cyprus, 1678 Nicosia, Cyprus*
[3)] *Department of Mechanical and Manufacturing Engineering, University of Cyprus, 1678 Nicosia, Cyprus*

[1)] sgkatz01@ucy.ac.cy

ABSTRACT

Reconfigurable structures show a great potential with regard to architectural developments that involve adaptive and interactive environments. The feasibility of integrating elementary robotics mechanisms in structural systems to achieve reconfigurability with minimum actuation means has been demonstrated in previous studies (Phocas 2019), (Phocas 2020). The lack of appropriate design codes for the structural design of reconfigurable structures, still poses a significant limitation to respective applications in practice. Structural design thus far, can be conducted based solely on the utilization of pertinent structural design codes for permanent, fixed-shape structures. However, well-targeted deviations from the recommendations of such structural design codes may be necessary to achieve efficient, but still safe designs, requiring significant engineering expertise. The present study aims to tackle this issue, demonstrating the structural design of a reconfigurable, temporary spatial structure by applying pertinent design codes for fixed-shape buildings. In this framework engineering assumptions that should be drawn beyond the design code recommendations, in order to fulfill requirements of reconfigurability, temporary nature, ease-of-erection etc., will be highlighted. Finite-Element Analyses of the simulated structure in two basic shapes, i.e., approximations of a paraboloid and an ellipsoid, are conducted to investigate its static and dynamic response. Load assumptions and design verifications are based on Eurocodes' recommendations, with any adopted related deviations being indicated and thoroughly discussed.

[1)] Postdoctoral Researcher
[2)] Professor
[3)] Assistant Professor

NOMENCLATURE

SYMBOL	UNITS	MEANING
Uppercase Latin		
$A_{Ed,ULS}$	N	design value of seismic action in an ultimate limit state
$A_{Ed,SLS}$	N	design value of seismic action in a serviceability limit state
C_e	-	exposure coefficient
C_t	-	thermal coefficient
E	N/m^2	modulus of elasticity
F_d	N	design actions
G	N/m^2	shear modulus
G_k	N	characteristic value of permanent action
I_u	-	turbulence intensity
Q_k	N	characteristic value of variable action
T_{lf}	years	design life
Lowercase latin		
b	m	building's width
c_{alt}		altitude factor
c_{dir}	-	directional factor for the estimation of v_b
c_e		exposure factor
c_o	-	orography factor
c_{pe}	-	external pressure coefficient
c_{pi}	-	internal pressure coefficient
c_{prob}	-	probability factor
c_r	-	roughness factor
c_{season}	-	season factor for the estimation v_b
f_o	N/m^2	characteristic value of 0.2% proof strength
f_u	N/m^2	characteristic value of ultimate tensile strength
g	m/s^2	standard gravity
h	m	buildings height
k_F	-	consequence factor
k_I	-	turbulence factor
k_r	-	terrain factor depending on the roughness length Zo
k_u	-	peak factor for turbulence
n_p	-	Ramberg-Osgood exponent
q_b	N/m^2	basic velocity pressure
q_p	N/m^2	peak velocity pressure
s	N/m^2	snow load
s_k	N/m^2	characteristic value of snow load on the ground for given location
v_b	m/s	basic wind velocity, defined as a function of wind direction and time of year at 10m above ground of terrain category II
$v_{b,0}$	m/s	fundamental value of the basic wind velocity
v_m	m/s	mean wind velocity
v_p	m/s	peak wind velocity

$v_{s,30}$	m/s	average propagation velocity of S waves in the upper 30 m of the soil profile at a shear strain of 10^{-5} or less
w_e	N/m^2	wind pressure
z	m	height for wind load estimation
z_0	m	roughness length
z_e	m	reference height for external pressure
Lowercase Greek		
a_{gR}	m/s^2	reference peak ground acceleration on type a ground
a_{par}	m	geometric parameter of the paraboloid
α_{th}	-	coefficient of thermal expansion
γ	-	specific weight
γ_G, γ_Q	-	partial factors for permanent and variable actions
μ_i	-	snow load shape coefficient
ν	-	Poisson's ratio
ρ	kg/m^3	density
$\rho_{o,HAZ}$, $\rho_{u,HAZ}$	-	reduction factors of f_o and f_u in the HAZ
σ_v	-	standard deviation of the turbulence
ρ_{wind}	kg/m^3	air density
ψ_0, ψ_1, ψ_2	-	Combination factors applied to a variable action to determine its combination, frequent and quasi-permanent value respectively

1. INTRODUCTION

Reconfigurable buildings emerge as pioneers in architectural innovation, steering a revolutionary shift toward dynamic structures capable of adapting to varying internal and external conditions. This transformative concept marks a departure from traditional static architecture, introducing an era where buildings can morph and optimize their shape in response to changing requirements. However, the realization of reconfigurable buildings presents intricate challenges, with structural design being of paramount concern. Unlike traditional static frameworks, reconfigurable buildings demand a structural paradigm capable of accommodating dynamic transformations while ensuring safety, stability, durability and functionality. This structural design challenge involves a spectrum of complexities, necessitating a respective approach to address the inherent dynamics of reconfigurable buildings.

Over the past decades, concepts of deployable and partially reconfigurable structures have been explored in various studies, such as in (King 1996), (Gantes 2001) and (Doreoftei 2014). Initially, the focus was on specialized structures designed for extraterrestrial applications, or on specific parts of static structures transforming into restricted forms. Related concepts were exemplified by retractable roofs as seen in (Ishii 2000) and (Jensen 2004). Recent research, however, has shifted towards the conceptualization of solutions, emphasizing reconfigurable buildings capable of transforming their shape based on user needs and adapting to various conditions, such as climate changes (Muresan 2020). This shift has gained momentum due to

advancements in digital and numerical technologies, as well as "smart" materials, promising upgraded aesthetics, improved climate behavior and enhanced practical functionality for contemporary architecture. Several studies in recent years have delved into architectural conception, kinematics and robotics to explore the development and potential applications of reconfigurable buildings. Previous studies conducted by (Christoforou 2015), (Phocas 2015), (Christoforou 2019), (Phocas 2019), (Phocas 2020), (Phocas 2022b) and (Christoforou 2023), aimed at designing systems of reconfigurable building structures, particularly focusing on lightweight, multi-joint bar linkage structures capable of sequential transformation through unlocking, exciting and locking individual joints, Fig. 1. The existing research has been predominantly verified in small scale experimental models using joint control components. Structural engineering considerations and kinematic conditions have been explored, assuming only rigid body motion.

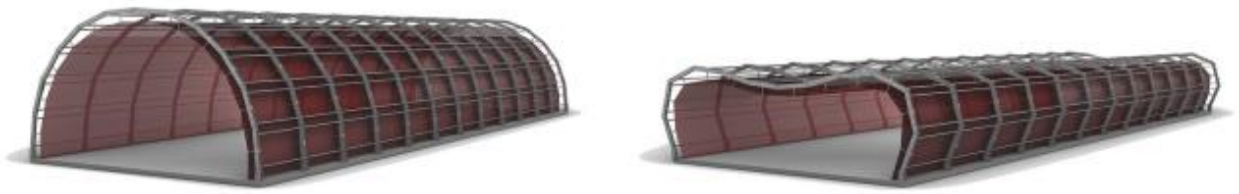

Fig. 1 Reconfigurable building structure of a rigid bar linkage system presented in (Phocas 2020)

Existing structural design codes are drafted for static buildings, posing a challenge for application to reconfigurable structures. Furthermore, the technology of reconfigurable buildings predominantly positions them as temporary, lightweight structures, adding complexity to the application of relevant design codes, unless appropriate engineering assumptions are made. The initial step toward safe design and practical realization of reconfigurable buildings involves static design for the less favorable shapes, based on current structural design principles.

Notably absent from the literature is also a thorough investigation into the structural design of reconfigurable structures for building applications. Despite previous structural analyses of similar, deployable lightweight structures (Gantes 1989), (Crisfield 2000), (Gantes 2001), (De Temmerman 2007), and even a case study of the structural design of a temporary structure according to Eurocodes (Koumar 2018), a comprehensive exploration of the structural design of reconfigurable buildings appears to be a novel endeavor. Preliminary analyses of internal forces in reconfigurable structures have been presented recently (Phocas 2022a), (Phocas 2024).

In this study, the structural design of a reconfigurable, temporary research pavilion is demonstrated, adhering to the provisions of the new generation of Eurocodes. The structure adopts a concept that employs robotics principles to reconfigure a multi-joint bar linkage system. The study aims at providing a detailed exploration of the structural design considerations for reconfigurable buildings. In particular, it includes irregularities encountered during the application of design principles for such structures, highlighting deviations that structural engineers should consider to ensure both economic and safe design.

2. RECONFIGURABLE, TEMPORARY STRUCTURE

2.1 Investigated scenario

The present study focuses on the design of a temporary and reconfigurable research pavilion with specific architectural requirements. The pavilion must be capable of safe and efficient deployment, reconfiguration and dismantling by a small group of users. Additionally, it needs to withstand diverse climatic and seismic conditions for universal applicability, with Greece chosen as the assumed country of application due to its elevated mean wind velocities and significant seismicity. The stochastic estimation of design loads, following Eurocode guidelines, considers Greece's unique wind, snow and seismic characteristics. Unfavorable values for certain parameters are intentionally chosen for a conservative approach, ensuring structural safety. However, to balance safety with economic and practical considerations, some design parameters receive more favorable values, preventing unnecessary increases in cross-section sizes and preserving the deployable nature of the structure. With the choice of Greece as the application country, the results may be further transferred to other European regions as well, with less challenging climatic and seismic conditions.

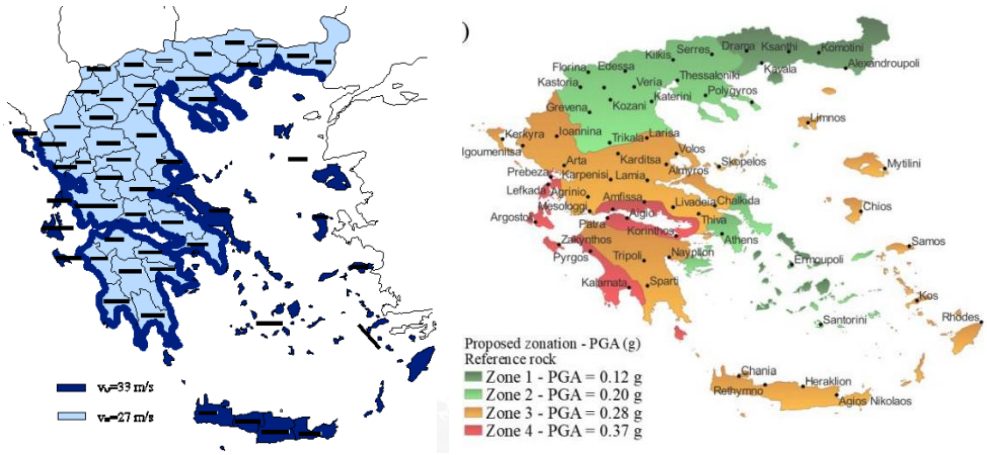

Fig. 2 Wind and seismic hazard maps of Greece (Malakatas 2015), (Pittilakis (2023)

2.2 Structural system

The proposed bearing structure consists of a lightweight system, featuring a central actuated telescopic pillar and eight systems of linkage bars. The individual bars have 1.0 m length, are evenly distributed and radially placed around the central pillar. The conceptualization of the structure refers to the vertical effective crank-slider approach explored in (Phocas 2021). In the early stages of conceptual design, a meticulous analysis led to the determination that a configuration of 16 bars on each radial axis, with 8 bars flanking each side of the central pillar, would be favorable in terms of the systems transformability attributes. The bars are assigned a CHS 219.1 x 10.0 cross section to EN 10210-2:2019. To enhance stability against horizontal loads, secondary bars of CHS 101.6 x 6.0 cross section to EN 10210-2:2019 interconnect the bar linkage systems in an axisymmetric pattern. All components of the bearing system consist of

structural aluminium EN AW 6061, as per EN 573-3:2004, in order to maximize the structure's lightweight characteristics. Detailed properties of EN AW 6061 are provided in Table 1. For the currently selected cross sections, the weight of each individual bar is 18 kg adding up to 28 kg, when reconfigurable nodes weight on either side of the bar is conservatively considered. Further increase in cross sections could be available, but limited as, based on recommended upper limits of safe weight lifting in the workplace (Hettinger 1981), (Staatssekretariat für Wirtschaft SECO 2023), an upper limit of 30 kg was set for individual components, to enable their lift by two humans, one male and one female and satisfy in this way above stated requirements regarding deployment and erection. Finally, for additional adaptability and to ensure the structure's lightweight nature, a THV membrane is envisaged for the building's envelope. This membrane will be mounted on auxiliary metallic mechanisms designed to accommodate reconfigurations without risking rupture or excessive loss of pretension.

Table 1 Physical and mechanical properties of EN AW 6061 (EN 573-3:2004)

γ	E	G	ν	α_{th}	f_o	f_u	$\rho_{o,HAZ}$	$\rho_{u,HAZ}$	n_p
[kN/mm^2]	[GPa]	[-]	[-]	[1/K]	[N/mm^2]	[N/mm^2]	[-]	[-]	[-]
26.48	70	27	0.296	$2.3 \cdot 10^{-5}$	110	180	0.86	0.83	8

The functionality of the structure involves multiple reconfigurations, prompting a preliminary static structural analysis in its initial design phase for the most critical ones. In this primary investigation, two principal configurations of a quasi-paraboloid and ellipsoid (i.e., characterized by a paraboloid and an ellipsoidal perimetric surface) were identified. The configurations were defined by the position vectors of the planar bar linkages, which include the internal joint angles of each linkage, as follows:

- $\Theta_{par,8} = [69.2, 154.9, 134.7, 171.0, 174.6, 175.8, 176.6, 176.9]^T$
- $\Theta_{ell,8} = [97, 154.9, 134.7, 171, 174.6, 175.8, 176.6, 176.9]^T$

The bearing system for these configurations is illustrated in Fig. 3. If the structural design were to progress solely based on static considerations, the methodology outlined below should be specifically applied to the most critical configurations, with further verification of the structure's safety during the reconfiguration process.

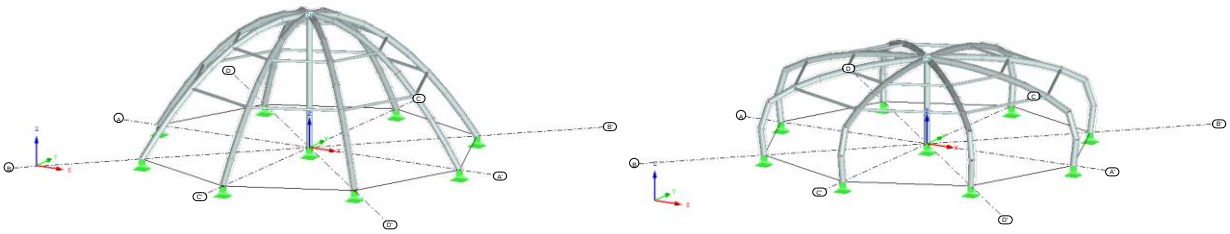

Fig. 3 Structural system in two configurations considered (isometric view)

3. STRUCTURAL DESIGN TO EUROCODES

The commercial Finite-Element (FE) software RFEM (Dlubal, 2023) was

employed for the current analyses, utilizing linear FE models with beam elements to represent the structure. The modeling approach involves neglecting the envelope of the building, as it is assumed to contribute negligible stiffness. Instead, its weight and loads are transferred to the load-bearing members of the structure. In this initial consideration, the reconfigurable joints were treated as continuous (moment-resisting) when locked. The current modeling choice results in a more rigid structure, and is expected to yield conservative results in terms of cross section and member verification, as each ray of the structure is treated as an individual member, substantially increasing its considered buckling length. Pinned connections of the bar systems and the central pillar to the ground are consistently accounted for in all cases.

3.1 Structure classification, design life and design parameters

In accordance with prEN 1990:2022, the structure is categorized as "Consequence Class 1 – Low" due to the anticipated minimal number of expected fatalities and the limited economic, social and environmental consequences in the event of failure. The design life T_{lf} for the structure is established at 10 years, aligning with the most conservative recommendation outlined in prEN 1990:2022 for temporary structures. This meticulous consideration of classification, design life and associated parameters ensures a thorough adherence to safety standards and temporary structure guidelines. The Ultimate Limit States (ULSs) of structural failure and loss of static equilibrium are considered in accordance with prEN 1990:2022. For the purpose of this study, other ULSs are disregarded, deeming them irrelevant. In the context of earthquake actions, Significant Damage (SD) Limit State and Limited Damage (LD) Limit State are respectively considered as Ultimate Limit State (ULS) and Serviceability Limit State (SLS) per prEN 1998-1-1:2022, Paragraph 4.3(1).

3.2 Considered actions and action combinations

The following permanent actions (G) are considered:

- Self-weight of structural members ($G_{k,sw}$) $= 26.48$ kN/m^3 (Table 1).
- Self-weight of THV membrane ($G_{k.env}$) $= 1980$ kg/m^3, which for a thickness of 500 μm equals to 0.99 kg/m^2 or 0.01 kN/m^2.
- Weight of reconfigurable joints ($G_{k.joints}$) $= 0.1$ kN (mass of appox. 10 kg).

The following variable actions (Q) are considered:

- Wind $(Q_{k,w})$ estimated to prEN 1991-1-4.
- Snow $(Q_{k,s})$ estimated to prEN 1991-1-3.
- Temperature $(Q_{k,T})$, estimated to prEN 1991-1-5.
- Seismic actions (A_E).

The fundamental and seismic combinations of actions were considered for the verification of the structure's ULSs. The accidental combinations are non-relevant, as no accidental action is considered at this stage. The characteristic, frequent, quasi-permanent and seismic design combinations of actions were considered for the

verification of the structure's SLSs. Equations detailing these combinations are provided in the ANNEX for clarity. Each combination is detailed with actions applied along the X or Y axes, in positive or negative directions and at maximum and minimum values (i.e., for Temperature actions) as required for a prudent estimation of the least favorable combination of actions. Given the axis-symmetry of the structure, only wind action parallel to the X-axis with a positive direction is taken into consideration. Additionally, snow is considered only in conjunction with the minimum temperature.

The following values for the partial and combination factors for buildings are considered:

- $\gamma_{G,\iota} = (1.215, 1)$ with the permanent action acting favorably and unfavorably respectively and for CC1 ($k_F = 0.9$).
- $\gamma_{Q,1} = (1.35, 1)$ with the variable action acting favorably and unfavorably respectively and for CC1 ($k_F = 0.9$).
- $\psi_0 = 0.5,\ \psi_1 = 0.2, \psi_2 = 0$, for snow actions, $\psi_0 = 0.6,\ \psi_1 = 0.2, \psi_2 = 0$, for wind actions, $\psi_0 = 0.6,\ \psi_1 = 0.5, \psi_2 = 0$, for temperature.

The chosen combination factors for snow actions align with the recommendations outlined in prEN 1990:2022, specifically suggested for applications at altitudes lower than 1000 m. Adopting less favorable values recommended for higher altitudes was deemed unnecessary.

3.3 Wind actions

Wind pressure distributions and their design values are estimated according to prEN 1991-1-4:2022. The wind velocity and pressure consist of a mean and a fluctuating component. The mean wind velocity is influenced by site-specific conditions, namely the wind climate and height variation, determined by terrain roughness and orography. Turbulence intensity I_u represents the fluctuating component. The structural response to across-wind dynamics is not considered. The mean wind velocity is determined by:

$$v_m(z) = c_r(z) \cdot c_o(z) \cdot v_b. \quad (1)$$

The significance of orography influence is considered significant and the less favorable terrain category is selected. Otherwise, the versatility of deploying the structure across various sites would be limited. Hence, peak velocity pressure is estimated using the following equation:

$$q_p(z) = \frac{1}{2} \cdot \rho_{wind} \cdot v_p^2\ (z), \quad (2)$$

External wind pressures are finally estimated based on equation:

$$w_e = q_p(z_e) \cdot c_{pe}, \quad (3)$$

Estimation of basic wind velocity v_b, peak wind velocity v_p, and reference height z_e were carried out according to prEN 19911-4:2022. To determine the shape and estimate values of wind pressure distributions, c_{pe}, as per prEN 1991-1-4:2022, both the paraboloid and the ellipsoid are regarded as domes with circular bases. In the second reconfiguration, the distribution of wind pressures on the perimetric surface below the ellipsoid is estimated as for vertical walls of a circular plan building following prEN 1991-1-4:2022, considering their inclination is approximately 5°. The outcomes of analytical estimations derived from equations

(1) to (4) and the estimation of c_{pe} have been included in the ANNEX.

3.3 Snow actions

Snow loads are estimated following prEN 1991-1-3:2022, treating them as static variable loads. The estimation of snow loads for persistent and transient design situations is expressed by the equation:

$$s = \mu_i \cdot C_t \cdot s_k. \quad (4)$$

Here, $s_k = 1.7$ kN/m^2 representing the less favorable value from Greece's map for snow loads (Malakatas 2015). The design parameters relevant to snow loads were carefully considered to meet the requirements of deployability and structural integrity. The following key considerations were taken into account:

- The structure's exposure to wind is assumed to be normal ($\mathrm{C_e} = 1$). Site-specific conditions should be considered for adopting a more favorable value corresponding to windswept conditions influencing snow deposition and by extension the respective loads, restricting applicability. Moreover, since the structure is intended to be deployed away from rural areas, less favorable values related to sheltered conditions were also deemed unlikely.
- The thermal transmittance parameter $\mathrm{C_t}$ is set to 1, so that the adopted value of the THV membrane remains on the safe side.
- While prEN 1991-1-3:2022 suggests special consideration for flexible envelopes prone to significant deformation under snow loads, the structure is treated as rigid. This decision is based on the understanding that the supporting mechanism of the membrane, forming the building's envelope, sufficiently contributes to its preservation under tension for non-exceptional snowfalls. Consequently, the structure is assumed to maintain its shape to a degree where load redistribution is negligible.
- In the event of heavy snowfall, the structure is envisioned to reconfigure into a near-conical shape with the maximum possible height and the smallest roof angle. This proactive measure aims to reduce the concentration of snow on the envelope. Notably, based on this assumption, no special considerations were made for exceptional snowfalls.

Two cases of snow load arrangement, a drifted and an undrifted, are considered for spherical domes as proposed by prEN 1991-1-3:2022, 7.2.6. The values of $s^{par} =$

3.4 kN/m^3 and $s^{ell} = 3.4$ kN/m^3 are calculated for the paraboloid and the ellipsoid respectively.

3.4 Temperature actions

The structural bearing members will be positioned entirely outside the building envelope, leading to the assumption of a uniform temperature distribution within their cross sections. Temperature extremes of 45°C and -5°C have been adopted as the most unfavorable values from the temperature map for Greece (Malakatas 2015).

3.5 Seismic actions

Seismic actions are assessed in accordance with prEN 1998-1-1:2022. The following considerations were made:

- The temporary character of the structure and the desire for universal applicability to a variety of sites, constitutes the selection of appropriate site category quite challenging. Site category C according to prEN 1998-1-1:2022 was considered conservative enough, as soft soils are quite rare in Greece. However, for a lightweight structure as the one investigated here, seismic actions are not expected to be predominant, so further considerations were avoided. An unfavorable value for the topography amplification factor was also adopted.
- The design of an aluminum structure of DC2 is prescribed based on the estimated seismic action index, referencing prEN 1998-1-2:2022, Table 15.4. Hence, for the current investigation, a behavior factor of q=2.5 is adopted, as specified in prEN 1998-1-2:2022, Table 15.1.
- Applying the updated seismic hazard map of Greece presented in (Pittilakis 2023), which incorporates the seismic actions $S_{a,475}$ and $S_{\beta,475}$ with a Return Period (RP) of 475 years, seismic actions for the current return periods of 275 and 100 years for the SD and DL are estimated considering the assumed CC to prEN 1998-1-1:2022.
- The structure is presumed to exhibit elastic behavior during a seismic event, leading to the adoption of the elastic design spectrum. The estimated values for the design elastic spectrum, denoted as $S_e(T)$, are provided in the ANNEX. Analyses, specifically focusing on the horizontal seismic components, indicated that the structural utilization under seismic loads is considerably lower compared to other Ultimate Limit State (ULS) combinations. As a result, the vertical component is deemed negligible and is consequently not considered in the analysis.

3.6 Analysis method

Linear elastic analysis has shown that Eq. (5)

$$\alpha_{cr} = \frac{F_{cr}}{F_{Ed}} \geq 10 \quad (5)$$

does not stand and hence, second order analysis has to be executed according to

prEN 1999-1-1:2021. Linear buckling analysis was carried out for both configurations and the 1st Eigenmode was applied as the unique, global and local, imperfection. To appropriately scale the eigenmode's shape, the equation recommended by prEN 199-1-1:2021 was omitted due to impractical complexity. Instead, the suggestion presented in (Vayas 2019) was adopted, stipulating that the magnitude of the imperfection should be equated to that of the local imperfection. This alternative approach was employed for practical feasibility. The local imperfection is estimated per prEN 1999-1-1:2021, $e_0/L = 0.0069$ m.

3.7 Deformation limits for the SLS verifications

The preliminary analysis series has revealed that adhering to the horizontal deformation limits recommended by Eurocode for non-reconfigurable and permanent buildings necessitates the adoption of relatively large cross sections. This, however, compromises the intended temporary nature of the structure. A prior study conducted by (Koumar 2018), addressing the structural design of barrel vault-shaped scissor structures for disaster relief purposes, introduced a more lenient acceptable limit of $h/100$ for horizontal displacement. In alignment with these findings and considering the expectation that deformations larger than those allowed by EN1990 for the characteristic combination would not result in damage to non-structural elements (such as the membrane) and given that the special character of the structure prioritizes user comfort and appearance less prominently, the same deformation limits are adopted in the present case as well. This decision is grounded in the unique requirements of the structure and its intended use, allowing for a more pragmatic approach to deformation limits. Therefore, horizontal deformations of up to $h/100 = 0.048$ m and $h/100 = 0.032$ m for the paraboloid and the ellipsoid respectively were considered acceptable.

4. ANALYSES RESULTS

4.1 Results of Lineal Buckling Analysis

The first two eigenmodes resulting from the linear buckling analysis, performed for the critical load combination (for the paraboloid: 1.22 x Self-weight + 1.35 x Wind X^+ + 0.68 x Snow drifted X^+ + 0.81 x T_{min}), are presented in Fig. 4. The critical load factor for the first four eigenmodes is $\alpha^1_{par,cr} = 4.146$, $\alpha^2_{par,cr} = 4.672$, $\alpha^3_{par,cr} = 4.908$, $\alpha^4_{par,cr} = 18.005$. In the 1st eigenmode the torsional movement of the structure around the central pillar is exhibited and corresponds to local imperfection of all members (bar linkage systems) in the counter-clockwise direction. The 2nd and 3rd eigenmodes were translational parallel to the two axes. Qualitatively similar results were obtained for the ellipsoid configuration as well, ($\alpha^1_{el,cr} = 3.519$, $\alpha^2_{el,cr} = 3.583$, $\alpha^3_{el,cr} = 3.615$, $\alpha^4_{el,cr} = 12.551$), with its first two eigenmodes being presented as well in Fig. 4.

.

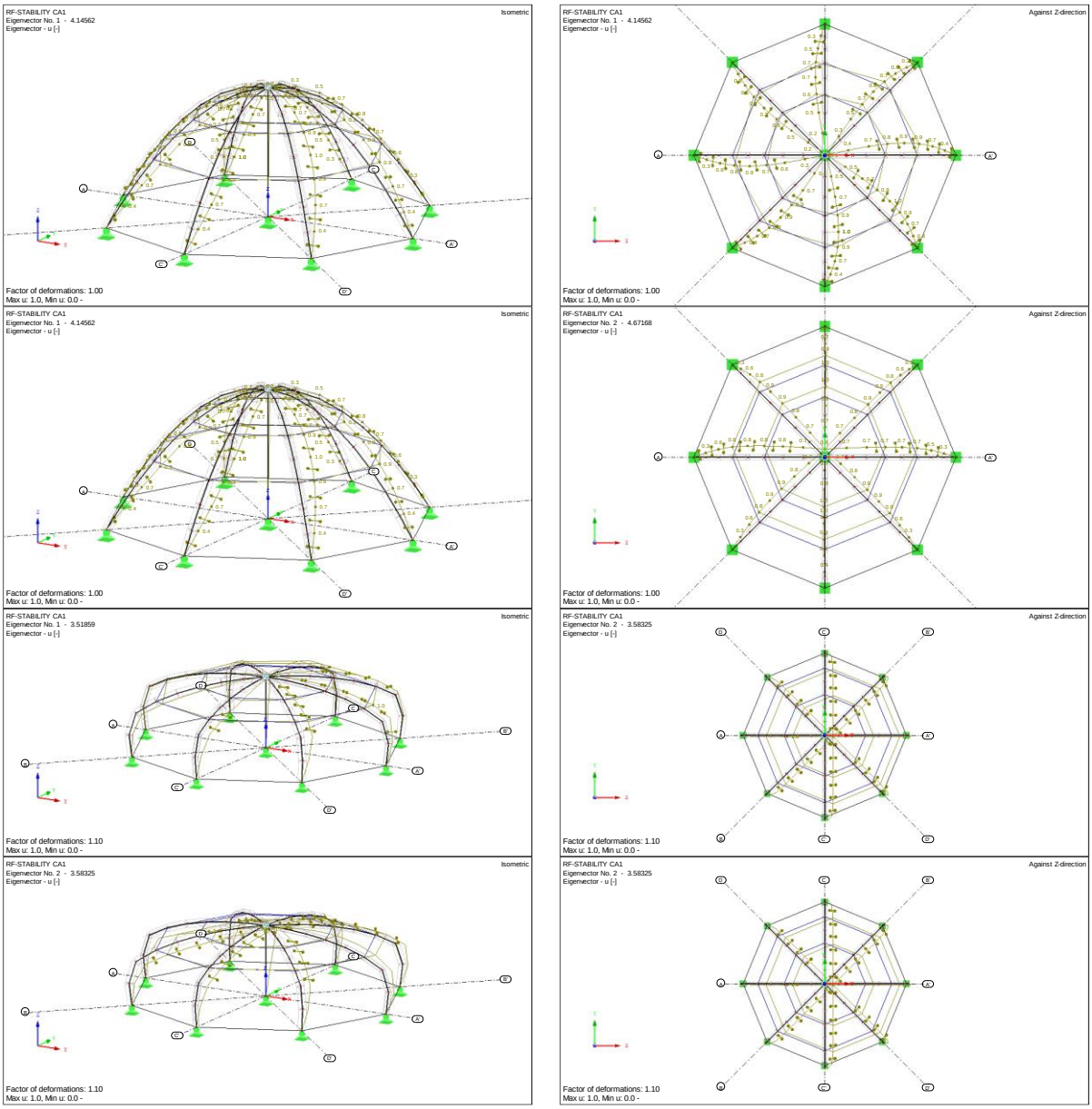

Fig. 4 Isometric and upper view of the first two buckling eigenmodes of the paraboloid (1st and 2nd line) and the ellipsoid (3rd and 4th line) configuration

4.5 Results of Geometric Nonlinear Analysis with Imperfections

With the execution of Geometric Nonlinear Analysis with Imperfections (GNIA), accounting for second-order effects in individual members and relevant imperfections, stress analysis alone is deemed sufficient for verifying structural durability and stability, eliminating the need for further member verification checks as per prEN 1999-1-1:2022. The envelope of estimated von Mises stresses, obtained through GNIA for the ULS verification cases, is presented for both paraboloid and ellipsoid configurations in Fig. 5. In both cases, the maximum von Mises stresses are below the limit $f_0/\gamma_{M0} = 110/1.1 = 100$ MPa. Specifically, for the paraboloid configuration, the maximum von Mises stress is 67 MPa, and for the ellipsoid, it reaches 94 MPa, resulting in a 27% increase in

structural utilization. Critical load combinations for the two configurations are provided. These results affirm that shape reconfiguration significantly influences structural behavior, underscoring the necessity for dynamic investigations to predict critical shapes and offer practical recommendations for the broader application of reconfigurable structures in real-life scenarios.

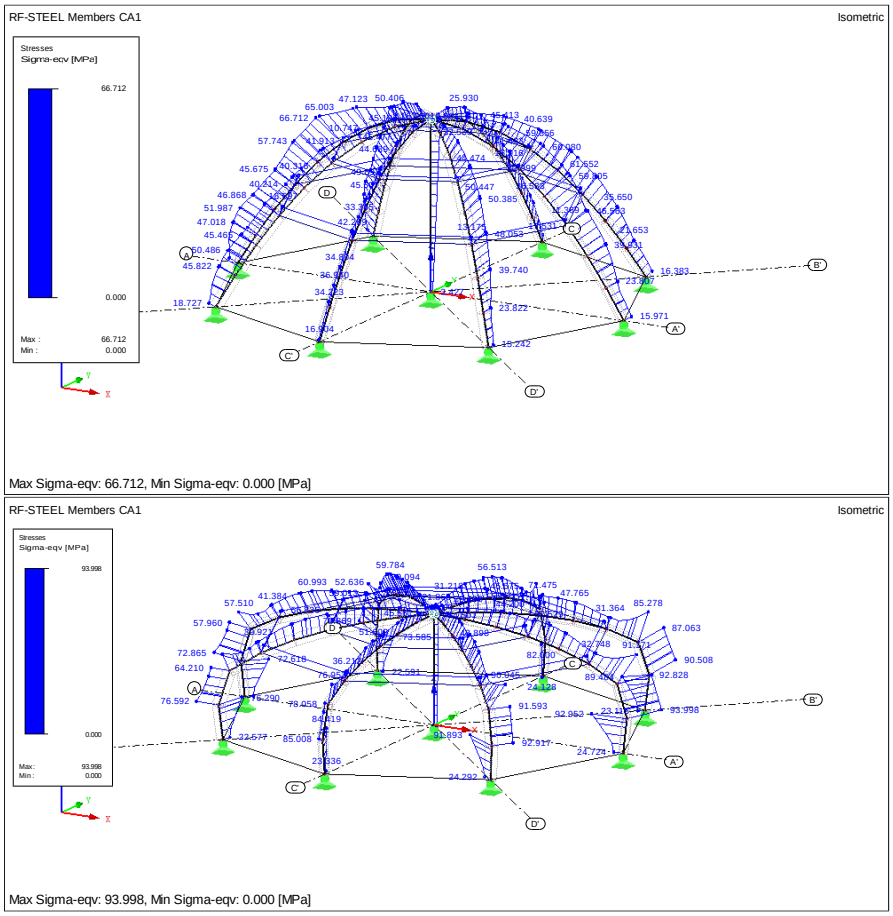

Fig. 5 von Mises stresses [MPa] of the paraboloid and ellipsoid configuration

The maximum horizontal displacements were documented for both configurations in the X axis direction, estimated at 36.3 mm and 34.1 mm for the paraboloid and the ellipsoid configurations respectively. For both configurations the critical SLS combination was the one with undrifted snow as the predominant variable load (1 x Self-weight + 0.6 x Wind X^+ + 1 x Snow undrifted). The result envelope of displacements along X are presented for both configurations in Fig. 6. Hence, for both configurations the deformations were within the acceptable limits. Vertical deformations were as well within the respective limits defined by Eurocode provisions.

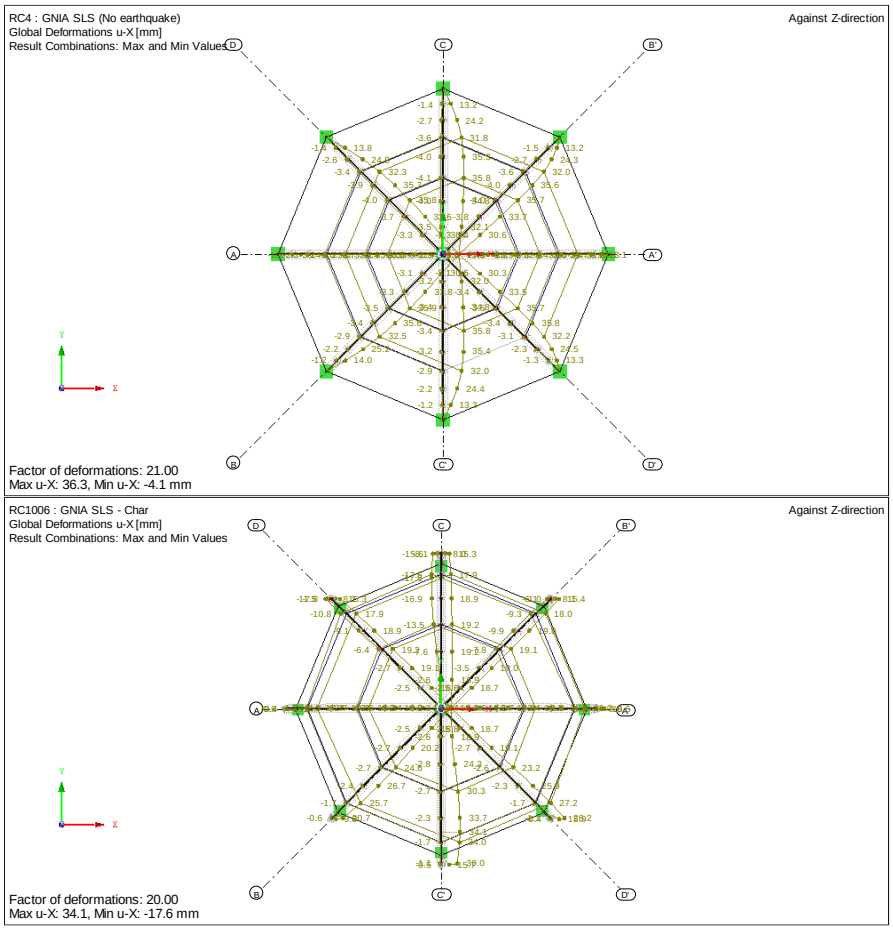

Fig. 6 Deformation in the X axis of the paraboloid (top) and ellipsoid configuration (bottom)

5. CONCLUSIONS

The current study explores the structural design of a reconfigurable, temporary research pavilion conforming to the latest Eurocodes. Designed for deployment in Greece, the pavilion's structural system involves a central pillar and strategically placed linkage bars for reconfigurability and structural stability. Employing numerical analyses, including Linear Buckling Analysis and Geometric Nonlinear Analysis with Imperfections, the study ensures a conservative yet economically balanced structural design. Special considerations that were made for the currently investigated temporary, reconfigurable spatial structure are summarized as follows:

- Individual components should not weigh more than 30 kgs to allow deployment by a pair of humans.
- Consequence class 1 was adopted due to minimal consequences in case of failure.
- Design life of 10 years, the least favorable value for temporary structures, was assumed.

- Deployment of the structure in the winter months was restricted to locations with altitude lower than 1000 m to reduce stochastic snow loads.
- Orography influence was considered significant and less favorable terrain category was assumed during estimation of wind loads so that universal application of the structure in several sites is possible.
- Site category C was selected for seismic action estimation as it was considered unfavorable for Greek conditions, although seismic combinations were not expected to be critical. This was confirmed due to the significantly lower structural utilization documented for the seismic combinations (11%) in regard to the critical. Further design iterations can be made for the least favorable site category F to check if the seismic combinations are not critical for this lightweight structure, even for worse site conditions.
- Horizontal deformation limits for SLS verification checks set by Eurocode for buildings were considered obsolete for the current type of structure. Less strict deformation limits were adopted.

The obtained results highlight the critical actions and combinations for the current and similar lightweight structures. Initial expectations about the significance of environmental loads and negligibility of seismic actions are confirmed. The present study ensured the designed pavilion's robustness in the investigated shapes retaining its temporary, deployable character, as the verified cross sections fulfill the requirements of lightweight limits set at the initial stages of the study. The need for further dynamic analyses of the structure against unexpected increases in internal forces during reconfigurations but also for pointing out the most critical shapes is becoming evident, due to the significant difference in structural utilization documented for the two investigated configurations. The presented methodology offers valuable insights and recommendations for practical implementation, catering to the needs of practitioners in the field.

ACKNOWLEDGMENT

The authors would like to acknowledge the ONISILOS and MSCA COFUND (Marie Skłodowska-Curie Grant Agreement No 101034403) for financing the research project DY.R.E.B., in the framework of which the present study was conducted.

REFERENCES

Christoforou, E.G., Müller, A., Phocas, M.C., Matheou, M. and Arnos, S. (2015), “Kinematics and control approach for deployable and reconfigurable rigid bar linkage structures”, *Trransactions of the ASME* **137**, 042302.

Christoforou, E.G., Phocas, M.C., Matheou, M. and Müller, A. (2019), “Experimental implementation of the ‘effective 4-bar method’ on a reconfigurable articulated structure”, *Structures* **20**, 157-165.

Christoforou, E.G., Phocas, M.C., Müller, A. and Georgiou, L. (2023), “A versatile reconfigurable mechanisms framework for applications in architecture”, *Journal of Intelligent & Robotic Systems* **20**, 157-165.

Crisfield, M.A. and Jelenić, G. (2000), “Finite Element Analysis and deployable structures”, Pellegrino, S., Guest, S.D. (eds) *IUTAM-IASS Symposium on Deployable Structures: Theory and Applications. Solid Mechanics and Its Applications* **80**.

Gantes, C.J. (2001), “Deployable Structures: Analysis and Design”, *WIT Press, Southampton Boston, 1st Edition.*

Gantes, C.J., Connor J.J., Locher D.R. and Rosenfeld, Y. (1989), “Structural analysis and design of deployable structures”, *Computers & Structures* **32** (3-4), 661-669.

De Temmerman, N. (2007), “Design and Analysis of Deployable Bar Structures for Mobile Architectural Applications”, Ph.D. Thesis, Vrije Universiteit Brussel.

Staatssekretariat für Wirtschaft SECO Schweiz - Direktion für Arbeit (2023) “Arbeitsbedingungen - Wegleitung zu den Verordnungen 3 und 4 zum Arbeitsgesetz”, veröffentlicht online, 31.07.2023.

Dlubal RFEM 6.0.5, academic license (2023), Dlubal Software GmbH, Tiefenbach, Bayern, Germany.

Doroftei, I., Doroftei, I.A. (2014), “Deployable structures for architectural applications - a short review”, *Applied Mechanics and Materials* **658**, 233-240.

EN 10210-2:2019, “Hot finished steel structural hollow sections - Part 2: Tolerances, dimensions and sectional properties”.

EN 573-3:2004, “Aluminium and aluminium alloys - Chemical composition and form of wrought products - Part 3: Chemical composition and form of products”.

Hettinger, T. (1981) “Heben und Tragen von Lasten – Gutachten über Gewichtsgrenzen für Männer, Frauen und Jugendliche”, *Bundesministerium für Arbeit und Sozialordnung, Berlin*.

Ishii, K. (2000), “Structural Design of Retractable Roof Structures”, WIT Press, Southampton, Boston.

Jensen, F.V. (2004), “Concepts for Retractable Roof Structures”, Ph.D. Thesis, University of Cambridge.

King, S.A. and Pellegrino, S. (1996), “Parametric excitation and dynamic instabilities in thin-walled deployable booms”, *Proceedings Spacecraft Structures, Materials, and Mechanical Testing*, 1153-1160, ESA SP-386, 27-29 March 1996.

Koumar, A., Tysmans, T and De Temmerman, N., (1995), “Structural design of barrel vault shaped scissor structures for disaster relierf”, *Journal of the International Association for Shell and Spatial Structures* **59**(3), 171-182.

Malakatas, N. (2015), “EN 1991 – Climatic actions & elaboration of maps for climatic actions in Greece”, *Elaboration of Maps for Climatic and Seismic Actions for Structural Design in the Balkan Region, Zagreb, 27-28 October 2015*.

Phocas, M.C., Christoforou, E.G. and Matheou, M. (2015), “Design, motion planning and control of a reconfigurable hybrid structure”, *Engineering Structures* **101**, 376–385.

Phocas, M.C., Christoforou, E.G. and Dimitriou, P. (2020), "Kinematics and control approach for deployable and reconfigurable rigid bar linkage structures", *Engineering Structures* **208**, 110310.

Phocas, M.C., Christoforou, E.G., Matheou, M. and Georgiou, N. (2024), "Kinematics approach and experimental verification of a class of deployable and reconfigurable linkage structures", *Structural Engineering* **150**(1), 04023206-1 – 04023206-14.

Phocas, M.C., Christoforou, E.G., Theokli, C. and Petrou, K. (2021), "Reconfigurable linkage structures and photovoltaics integration", *Building Engineering* **43**, 103201-1 – 103201-12.

Phocas, M.C., Georgiou, N. and Christoforou, E.G. (2022a), "A class of actuated deployable and reconfigurable multilink structures", *Advances in Computational Design* **7**(3), 189-210.

Phocas, M.C., Matheou, M. and Haase, W. (2022b) "Transformable building structures in architectural engineering education", *Architecture, Structures and Construction* **2**, 183–198, 2022.

Phocas, M.C., Matheou, M., Müller, M. and Christoforou, E.G. (2019), "Reconfigurable modular bar structure", *Journal of the International Association for Shel and Spatial Structures* **60**(1), 78-89.

Pittilakis, K., Riga, E. and Apostolaki, S. (2023), "Proposal for a new seismic hazard zonation map for Greece", 3rd European Conference on Earthquake Engineering & Seismology, Bucharest, Romania, 2022.

prEN 1990:2022 "Basis of structural and geotechnical design", draft March 2022.

prEN 1991-1-3:2019 "Actions on structures - General actions – Snow loads", draft October 2019.

prEN 1991-1-4:2024 "Actions on structures - General actions - Wind actions", draft March 2023.

prEN 1991-1-5: 2023 "Actions on structures - Thermal actions", draft March 2023.

prEN 1998-1-1: 2022 "Design of structures for earthquake resistance – General rules, seismic actions and rules for buildings", draft September 2022.

prEN 1998-1-2: 2022 "Design of structures for earthquake resistance – Buildings", draft December 2022.

prEN 1999-1-1:2021 "Design of aluminium structures – General structural rules", draft March 2021.

Vayas, I., Ermopoulos, J. and Ioannidis, G. (2019) "Design of Steel Structures to Eurocodes", *Springer Tracts in Civil Engineering, Springer Nature, Cham, Switzerland*.

ANNEX

A.1 Combinations of actions

Fundamental combinations: $\sum F_d = \sum_\iota \gamma_{G,\iota} \cdot G_{k,1} + \gamma_{Q,1} \cdot Q_{k,1} + \sum_{j>1} \gamma_{Q,j} \cdot \psi_{0,j} \cdot Q_{k,j}$

Seismic combinations: $\sum F_d = \sum_\iota G_{k,1} + A_{Ed,ULS} + \sum_{j>1} \psi_{2,j} \cdot Q_{k,j}$
Characteristic combinations: $\sum F_d = \sum_\iota G_{k,1} + Q_{k,1} + \sum_{j>1} \psi_{0,j} \cdot Q_{k,j}$
Frequent combinations: $\sum F_d = \sum_\iota G_{k,1} + \psi_{1,j} \cdot Q_{k,1} + \sum_{j>1} \psi_{2,j} \cdot Q_{k,j} + P_k$
Quasi-permanent combinations: $\sum F_d = \sum_\iota G_{k,1} + \sum_{j>1} \psi_{2,j} \cdot Q_{k,j} + P_k$
Seismic design combinations: $\sum F_d = \sum_\iota G_{k,1} + A_{Ed,SLS} + \sum_{j>1} \psi_{2,j} \cdot Q_{k,j} + \gamma_P \cdot P_k$

A.2 Estimated wind action design values

Estimation of $c_{pe.10}$ for the paraboloid shape (see prEN 1991-1-4:2022, Fig. C.30):

$$\begin{cases} \dfrac{f}{d} = \dfrac{4.808}{12} = 0.4 \\ \dfrac{h}{d} = 0 \end{cases} => \begin{cases} Zone\ A: c_{pe.10} = 0.65 \\ Zone\ B: c_{pe.10} = -1 \\ Zone\ C: c_{pe.10} = 0 \end{cases}$$

Estimation of $c_{pe.10}$ for the ellipsoid shape (see prEN 1991-1-4:2022, Fig. C.30):

$$\begin{cases} \dfrac{f}{d} = \dfrac{1.21}{12} = 0.10 \\ \dfrac{h}{d} = \dfrac{1.943}{12} = 0.16 \end{cases} => \begin{cases} Zone\ A: c_{pe.10} = -0.43 \\ Zone\ B: c_{pe.10} = -0.45 \\ Zone\ C: c_{pe.10} = -0.16 \end{cases}$$

Results:	Comments:
$c_{prob} = 1,\ c_{dir} = 1,$	recommended values in prEN 1991-1-4, 6.2(2)
$c_{season} = 1,\ c_{alt} = 1$	structure can be used at any time of the year
$v_{b,0} = 33$ m/s, $v_b = 33$ m/s	Greek basic wind velocity map, coastal areas
$z_{par} = 4.808,\ z_{ell} = 3.153$	height of building in the two basic reconfigurations
$z_0 = 0.003,\ z_{min} = 1$	EN1991-1-4, Table 4.1, Terrain category 0
$k_r = 0.156$	
$c_r^{par}(z) = 1.1515,\ c_r^{ell}(z) = 1.0856$	
$c_o(z) = 1.48$	less favorable value in prEN 1991-1-4 ANNEX A3
$v_m^{par}(z) = 68.39$ m/s, $v_m^{ell}(z) = 64.48$ m/s	
$I_u^{par}(z) = 0.0753,\ I_u^{ell}(z) = 0.0798$	
$k_u = 2.8$	recommended value in prEN 1991-1-4, 6.5(1)
$v_p^{par}(z) = 82.81$ m/s, $v_p^{ell}(z) = 78.90$ m/s	
$\rho_{wind} = 1.25$ kg x m^{-3}	recommended value in prEN 1991-1-4, 6.2(5)
$q_p^{par}(z) = 3120.1,\ q_p^{ell}(z) = 2842.5$	
$c_{pe}^{par} = (0.65, -1, 0),\ c_{pe}^{ell} = (-0.43, -0.45, -0.16)$	estimated above
$w_e^{par} = (2.028, -3.120, 0),\ w_e^{ell} = (-1.22, -1.28, -0.45)$	

A.3 Estimated elastic response spectrum values

Estimated data:	Comments:
$T_{SD,CC1} = 275$ years	return periods for SD LS and DL LS for CC1, see prEN
$T_{DL,CC1} = 100$ years	1998-1-2:2022, Table 4.3
$\delta = 0.6$	see prEN 1998-1-2:2022, Table 4.2
$v_{s,30} = 580$ m/s	mean value for ground type C from EN1998-1-1:2006
$S_{a,475} = 0.92 \cdot g = 9.03$ m/s^2	less favorable values in the Greek seismic map

$S_{\beta,475} = 0.34 \cdot g = 3.34$ m/s^2
High seismicity level is selected according to to prEN 1998-1-1:2022
$F_a = 1.306,\ F_\beta = 2.065$ see prEN 1998-1-1:2022, Par. 5.2.2.2(5) and (10)
$F_T = 1.4$ topography amplification factor, less favorable value to prEN 1998-1-1:2022, Par. 5.2.2.2, Table 5.5
$T_\beta = 1$ s see prEN 1998-1-1:2022, Par. 5.2.2.2(1)
$S_\delta = 9.9$ m/s^2 > 6.5 m, classification as high seismic action DC2 is applied see prEN 1998-1-1:2022, Table 15.4
$S_a = 16.50$ m/s^2, $S_\beta = 9.64$ m/s^2, $T_A = 0.02$ s, $F_A = 2.5$, $\chi = 4$ see prEN 1998-1-1:2022, Par. 5.2.2.2(2)
$S_a/F_A = 4.53$ m/s^2
$T_C = \frac{S_\beta \cdot T_\beta}{S_a} = 0.58$ s see prEN 1998-1-1:2022, Par. 5.2.2.2(2)
$\frac{T_C}{\chi} = 0.22$ s, $T_B = 0.1$ s, $T_D = 1 + S_{\beta,475} = 4.34$ m/s^2
$\eta = 1$ damping correction factor for 5% damping ratio